

NEW VACUUM SENSOR FOR DETECTING SURFACE CRACKS ON WELDS

Choi C H

ABSTRACT

A new vacuum sensor is very effective at detecting initiation and growth of cracks on weld surfaces. This sensor operates by detecting small changes of pressure when a crack passes under an evacuated cavity. Because the system relies on vacuum for detection of defects, it is independent of the other factors such as material, mechanical, and electrical properties that might otherwise affect sensor systems. For this reason, the sensor is largely free from boundary conditions. The only exception to this rule is that the sensor is sensitive to geometric effects such as the weld 'ripple'.

It is demonstrated that the technique can reliably be used to determine crack size, and thereby anticipate fracture type as well as future service life.

KEYWORDS

Vacuum sensor, Adhesives, Weld, Cracking ,Pressure, Fatigue, Weld monitoring and Fracture.

AUTHOR DETAILS

Dr Choi works for Maritime Platform Division at Defence Science and Technology Organisation in Melbourne as a sensor researcher.

1. INTRODUCTION

Weld zone hydrogen cracking is a key concern in the fabrication of thick section weldments in high yield stress steels because the cracking is commonly formed and difficult to detect. There is therefore a significant risk of structural failure when cracking exists. Management of cracking can be achieved by non-destructive examination, however, extremely advanced Non-Destructive Inspection (NDI) techniques [1,2] are normally required to find and characterise these cracks properly so that the risk of cracking is minimised.

Rather than rely on a programme of extensive non-destructive inspection, this work hopes to identify a cost-effective system based on sensors that can give off an alarm before the surface crack reaches a critical level. Five sensor techniques are being investigated by Maritime Platforms Division (MPD). They are strain gauges [3,4], vacuum sensors [5], optical fibres [6,7,8], piezoelectric sensors [9,10,11,12], and the Micro-electro Mechanical System [13,14] (MEMS)-connected pressure sensor. This report examines and evaluates the capabilities of one of the sensors: the SMS vacuum sensor. The system under investigation was developed by the Structural Monitoring System Co and is covered by an International Patent Application (No. PCT/AU/00235) [5]. SMS Co. worked with MPD on this project.

1.1. The Sensor

The vacuum sensor was originally developed for monitoring of airframes and has potential application for bridges and buildings and thick walled, welded structures, such as pressure vessels. The system is known to be accurate with high sensitivity for detecting surface cracks. It still requires further development however, before it can be considered reliable enough for health monitoring purposes.

The SMS sensor is a continuous vacuum system, which is operated with a rotary pump to measure and analyse the pressure status inside a vacuum channel. The size of this pump is a critical issue. In a confined-space area such as tanks on a naval vessel, it is essential to minimise the size of the sensor as much as possible.

The current work is aimed at analysing transverse cracks on welds by modifying and applying the SMS vacuum system so that this sensor can be used for permanent in-situ health monitoring of welds in the hull.

2. FUNDAMENTAL PRINCIPLE OF THE VACUUM SENSOR

The principle of the sensor is shown in Figure 1. It comprises four main elements: a vacuum source, calibrated flow impedance, self-adhesive sensor pads (vacuum channels), and a differential pressure monitor.

A steady state vacuum is maintained in a Sensor Cavity (refer to Figure 1.) by means of a high impedance connecting duct attached to a constant vacuum source. Any airflow through the high impedance duct creates a pressure drop across the duct and is sensed by the differential pressure sensor.

Users can select single or manifold channel techniques arbitrarily. On the side of the sensor pad being applied to the weld surface the sensor pad sheets have an engraved pattern of parallel, interlaced, micro-channels arranged into manifolds, kept at atmospheric pressure and the system vacuum pressure respectively. That is, every alternate channel is evacuated. The geometric size and shape of a sensor pad, and the size and configuration of its manifold channels, will depend on the shape of the object to be monitored, its location, and the material it is made from.

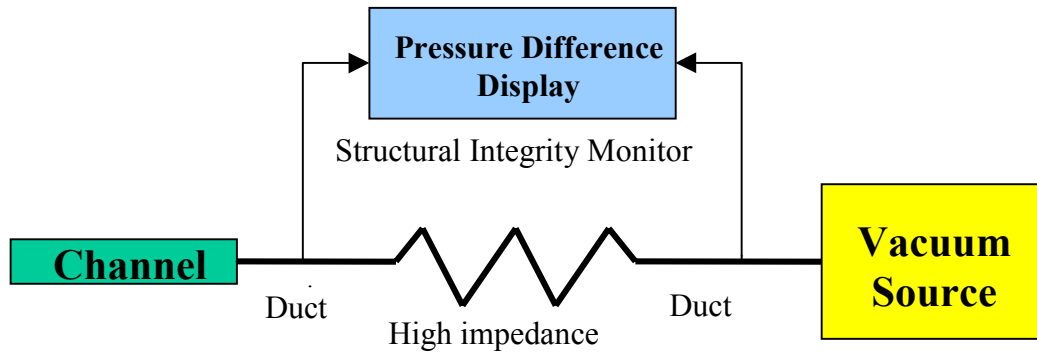


Figure 1.

Any crack appearing on the surface, which crosses from one evacuated channel to an adjacent channel will trigger a measurable deterioration in the vacuum of the sensor, whilst the flow impedance keeps the pressure at the vacuum source virtually constant.

Due to this shift in vacuum balance, the differential pressure monitor is able to signal the appearance of the crack.

3. EXPERIMENTAL

Vacuum sensors were attached to two types of test coupons. One type of coupon was fabricated from mild steel without weld (MSWW) and a second, more complex, type of coupon was fabricated from high strength BIS-812-EMA steel with T-butt weld (BESWW). Figures 2a and 2b contain the coupon designs as well as the location and orientation of the attached vacuum sensors. Sixteen coupons were prepared for MSWW and two for BESWW.

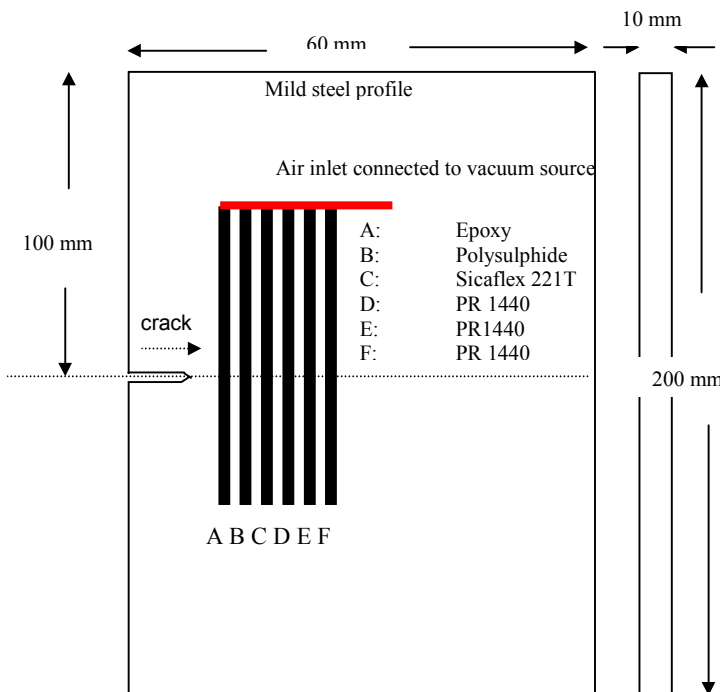


Figure 2a.

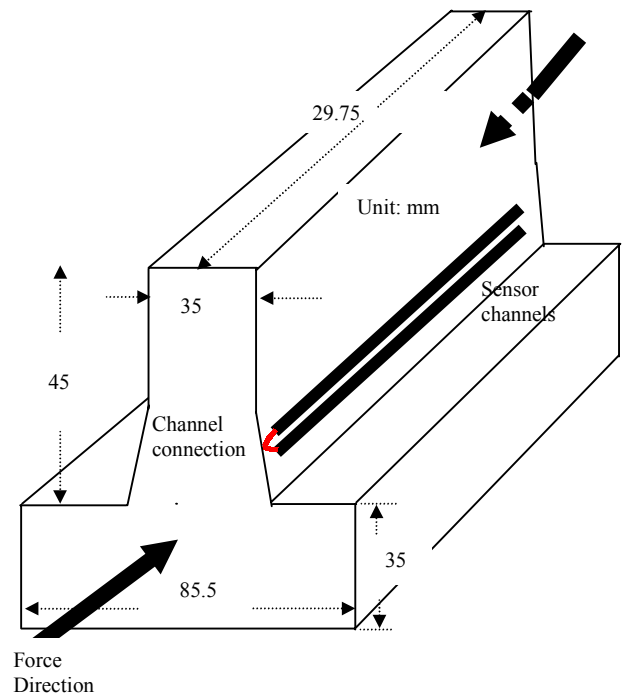


Figure 2b.

Three of the coupons (MSWW Type) were coated with primer paint to check the stability of the vacuum sensor cavity. The samples were coated with Intergard EGA088/EGA089 with an average film thickness of 88 μm .

Two hydraulic fatigue machines with maximum tensile force of 100 kN and 2 MN, respectively, were used to test the MSWW coupons and a BESWW coupon. The load conditions are detailed in Table 1 for the F1 and F2 series samples.

To test the environmental performance of the sensor pads, 6 silicone tubes were attached to the F2-1 sample. The sample was monitored for 2 days under no load conditions to check for gas leakage and duct blocking along the cavity of the vacuum sensor. To test the performance of the bond between the weld surface and vacuum sensor cavity a variety of adhesives were used. These were PR 1440, Sicaflex 221T, polysulphide, and epoxy.

Furthermore, 6 MSWW coupons (F5 series) with vacuum sensors attached were stored in an open container under 1 atmosphere for six months and 1 year to check material permeability and adhesiveness, respectively. The specimens were checked on a monthly basis. Upon completion of each permeability and adhesion test, the samples were returned to the container.

Table 1.
Load Conditions for F1 and F2 Series Samples

Sample (number)	Maximum Load (kN)	Minimum Load (kN)	R (Max./Min) ratio
F1-2 (2)	55	0	0
F2-1 (2)	55	5.5	0.1
F2-2	60	6.0	0.1
F2-3	70	7.0	0.1
F2-4	55	7.0	0.1
F2-5 (2)	110	11	0.1
F2-6	120	12	0.1
F2-7 (2)	100	10	0.1
F2-8	50	5	0.1
F2-9	70	7	0.1
F2-10a	50	0	0.1
F2-10b	60	0	0.1
F2-10c	70	0	0.1

The F3-1 test coupons were subjected to a compressive force as shown in Figure 2b. The centroid point of the T-Butt coupon was calculated and a special jig was manufactured to ensure that the centre of the MTS piston coincided with the calculated centroid of the T-Butt coupon in an attempt to minimise possible buckling effects during the cyclic loading. The maximum compressive load for the MTS machine was limited to 1.5 MN. Two parallel line cavities separated by 1cm were attached to the surface of the weld. A silicone tube was used to connect one end of the cavity to the adjacent end of the parallel cavity as shown in Figure 2b. This configuration was used on each side of the T-Butt coupon.

A Delogpro program created by Data Electronic Company was used for collecting channel pressure output via a Datalogger connected to a PC. Differential pressure measurements between the vacuum source and the sensor channels were determined using the differential pressure monitor at 1 mbar = 20mV .

Four different types of adhesives were used to attach the sensor cavities on each coupon to check the durability of the sensor pad. Six coupons were stored in an open container under normal atmosphere for periods ranging from 3 months to 1 year.

4. RESULTS AND DISCUSSION

4.1. Adhesive Bond Performance

After three months, three coupons were examined by optical microscopy to determine the condition of the adhesive bonds. No discernible bondage break was found during this period. It was noted, furthermore, that none of the coupons under investigation showed any significant deterioration of the bond after one year.

4.2. Alarm Sensitivity

The fatigue test coupons were prepared in accordance with the international (ASTM) fatigue test standard. To obtain an optimum load condition for the F2 series test coupons, a gradually increasing tensile force was applied to a sacrificial coupon. At a tensile force of 55 kN Lüder's band started to appear near the tip of the crack machined into the coupon as shown in Figure 3. The load was gradually increased to 120 kN until the Lüders band crossed the width of the coupon. From an engineering viewpoint, the initial stage of Lüders band was regarded as the starting point of plastic flow. The propagation angle of Lüder's band is shown as dotted line in Figure 3.

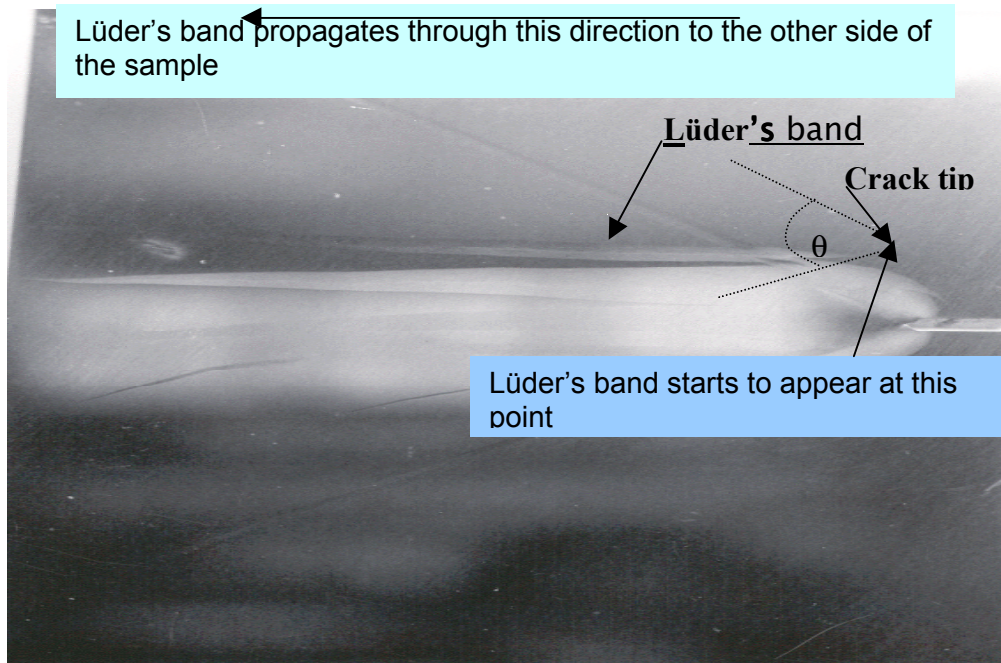


Figure 3.

It was found during these initial tests that the alarm sensitivity of a vacuum sensor was not affected by factors such as crack propagation rate, load condition, and number of load cycles unless a crack reaches the front edge of the sensor cavity. For this reason, the fatigue amplitude was arbitrarily set between 55 kN to 120 kN with the frequency range between 5 Hz and 10 Hz.

The rate of crack growth was kept below 50000 cycles/mm by controlling the load when the crack reached the channel line under investigation. The initial stage of crack propagation through the channel could be measured and analysed precisely by this technique.

As stated previously, under zero load conditions the four adhesives did not show any leakage during the test period. To investigate the performance of the adhesives when subjected to dynamic loading, fatigue tests were performed on three coupons (F10 series). All of the adhesives performed well and none showed adhesive bond breakage along the interface between the cavity and weld after 200,000 cycles at a range between 50 to 70 kN. Testing of the adhesives over a longer period is required to identify the adhesives that demonstrate the best performance.

4.3. Alarm Pressure

When a crack crossed the sensor pad (cavity channels), air flowed into the SMS sensor at a greater rate than the normal permeability flow of the channels. An increased differential pressure indicated that a change in the flow rate of air had occurred.

To determine the alarm pressure threshold, a small silicone cavity with a diameter of 250 μm sealed on a plastic substrate was prepared. A small sharp crack was created by a knife near the centre of the sample length. . An artificial crack was forced to travel from this knife cut and pass through the cavity very slowly by gradually increasing the tensile load and observing the pressure. By trial and error, an alarm pressure threshold of 1.37 mbar was chosen because the signal data due to electrical noise at this level could be visibly separated from the signal data due to the crack.

4.4. Calibration

The F2-5 sample has six SMS sensors, A, B, C, D, E, and F, vertically located from the centre edge, (refer to Figure 2a. above) and these are connected by a gas inlet tube. The sample was fractured after 300,000 load cycles

Figure 4. shows voltage deviation against crack growth at the stage at which a crack crosses the edge of sensor A. The load regime cycled between a maximum 110 kN and a minimum 11 kN cyclic at a frequency of 10 Hz It took 36 seconds from the time of initial gas leak to the time the alarm was activated. It is evident in Figure 4 that the air inside the sensor tube started to leak just below the preset alarm threshold.

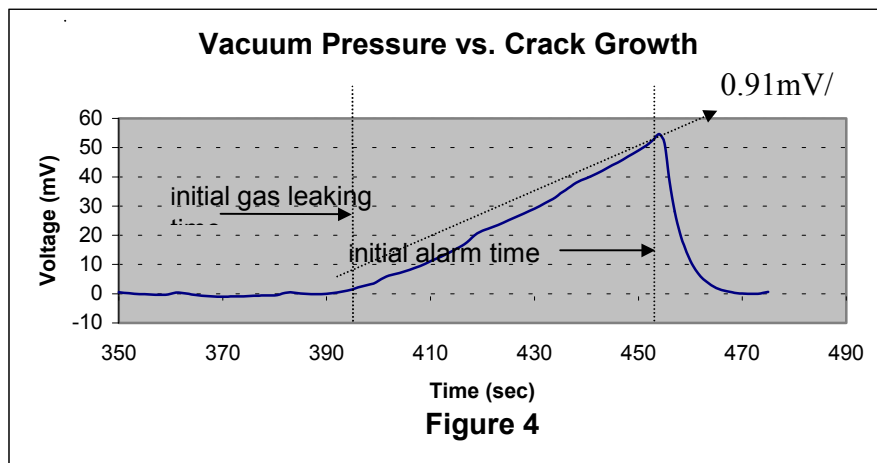
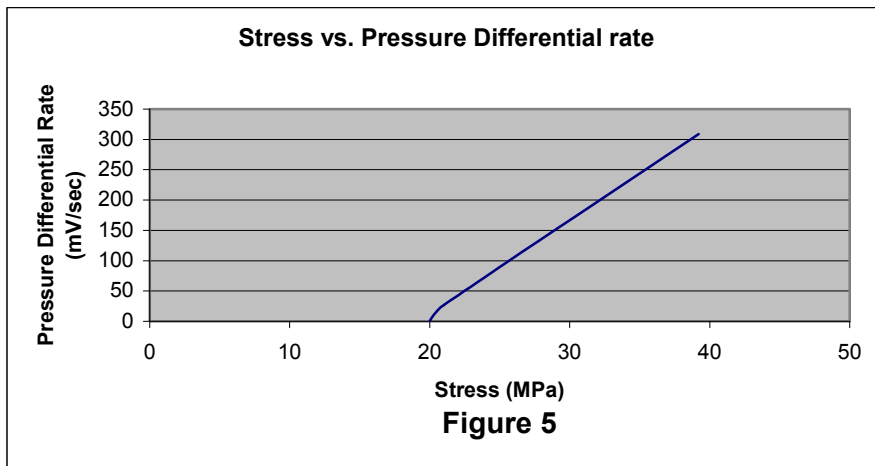


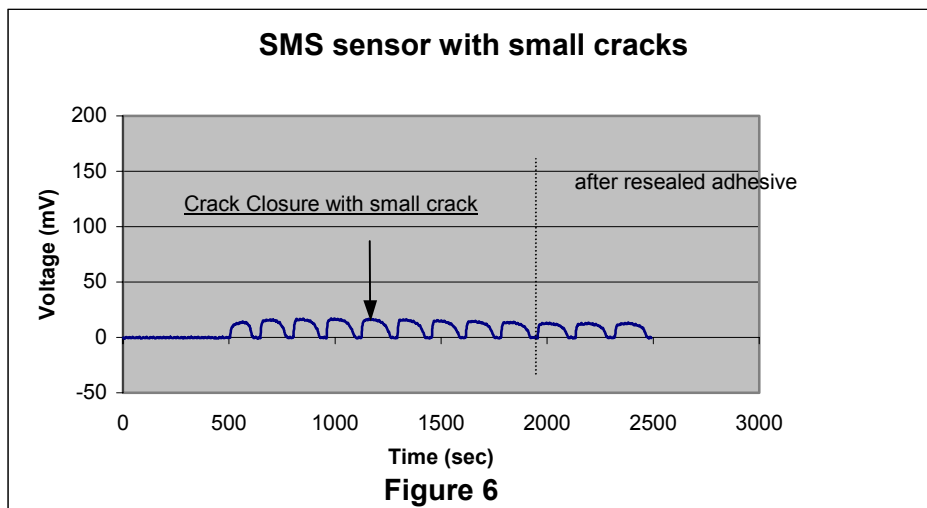
Figure 4. shows that the gradient of voltage time curve was 0.91 mV/sec at a time when the crack crossed sensor A.. As the crack continued to grow the real cross-section of the coupon was reduced so that the stress over the coupon was redistributed. Whenever a crack crossed through a channel, the experiment was stopped and the channel was blocked mechanically so that it no longer leaked air. The experiment then proceeded for the remaining sensors (B, C, D, E, and F) to also study the effects of stress against pressure differential rate (mV/s). Figure 5 shows clearly the relationship between pressure differential rate and stress. The gradient was increased from 0.91 mV/sec at 20 MPa up to 300 mV/sec at 40 MPa.



It is worth noting that the stress variation in Figure 5. is directly related to the change of the real sample area due to the growth of the crack. In other words, the vacuum sensor system can be used to monitor crack growth as well as for identifying the existence of a surface crack

4.5. Crack Closure Events

Owing to the plasticity of mild steel near a crack tip, crack closure effects can occur in these specimens. These effects were investigated by controlling the cyclic load imposed on the test coupon F2-8 at the stage of crack initiation. The data sampling interval was reduced to 5 Hz at 5 Hz cyclic loading. The load was cycled between a maximum load of 50 kN with a load ratio (max/min load), R, of 0.1. Under dynamic tensile load, the crack remains open. When the loading goes to the minimum however, the output voltage drops to zero Figure 6. shows repeated crack closure indicated by a constant voltage drop to zero volts. It assumed that the crack is stable at this stage (that is, a crack is not growing at this stage).



It is important that one can estimate the maximum force/stress that can be tolerated before a crack grows and thus create a maximum safe threshold envelope. This was done by increasing the load gradually until the voltage went up continuously. At this stage, the crack closure phenomenon will disappear and the crack propagation will speed up.

4.6. Adhesive Repair of Sensors

The accuracy of the results obtained from the vacuum sensor could be affected by the adhesive entering the sensor cavity.

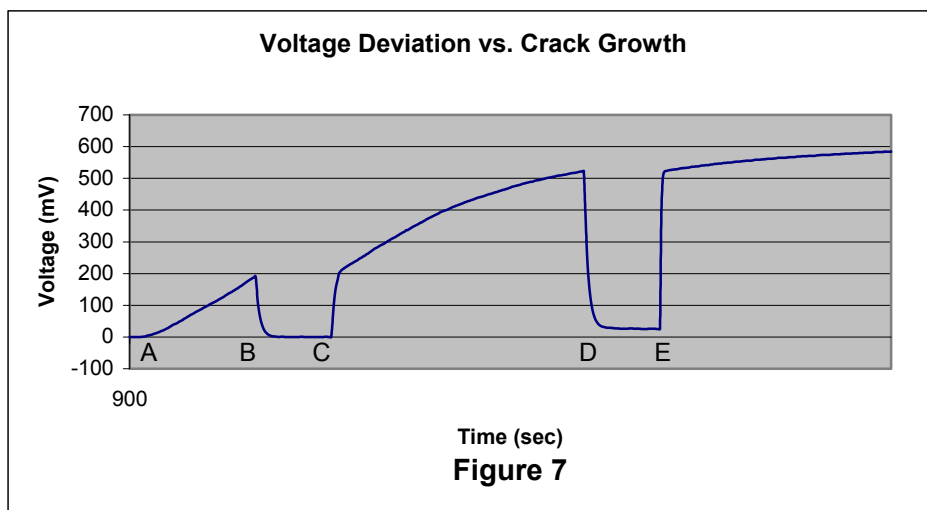
In an attempt to determine the effect that adhesives may have on crack closure, part of the adhesive around the vacuum sensor cavity, which is strongly bonded on the crack tip of test coupon F2-8, was carefully peeled off. The area was then cleaned thoroughly and sealed again using the same adhesive. Great care was taken to avoid blocking the inside of the cavity. The tests were then restarted and the results before and after the repair were compared. The vertical dotted line in Figure 6. defines the results before and after the sensor was sealed and resealed on the sample. There was no noticeable change in output voltage before and after the repair. This test was repeated 5 times. Since the adhesive was demonstrated to be working efficiently, even after repair, it is reasonable to assume that the voltage drop during the rest period may be caused by the crack closure effect.

4.7. Characterisation of Cracking

These results illustrate that the test procedure can provide additional information about the nature of cracking in the specimen. In particular, the threshold of the tolerable crack propagation rate can be accurately anticipated just by observing the output data and the intermittent pattern of signals as shown in Figure 6. For fast growth of a crack, beyond this threshold, the signal goes up constantly. This can be easily distinguished from intermittent cracking that shows closure effects. To illustrate this, Sample F2-9 was used for a test and the results are shown in Figure 7. The maximum and minimum loads were 70 kN and 7 kN, respectively, at 5 Hz cyclic loading and 5 Hz sampling rate.

Figure 7. shows the relationship between voltage and time during the growth of a particular crack (F2-9). The line between A and B in Figure 7. shows the voltage change due to the pressure deviation as the crack tip approached the edge of the first vacuum channel. It is almost a linear relationship. There was a rest period between B and C. As the crack progressed through the coupon after C the cross section of the coupon was reduced and the stress increased thereby contributing to an increase in the rate of crack growth. The voltage therefore increased with time and this demonstrated that the crack length was increasing. The relationship between pressure and voltage however, did not exhibit a linear relationship i.e. the voltage continued to increase but the rate of increase reduced. It is notable that during a second rest period from D to E that the voltage did not return to zero, implying that the crack remained open at this stage.

Another observation is that the gradient of the pressure difference can be used as an indicator of how much air/or gas leaked volumetrically during the period that an examiner decided. It further suggests that with these gradients, one can calculate the crack growth accurately. Slow crack growth is typified by a gentle gradient whereas fast crack growth is characterised by a steep gradient.



4.8. Application to a T-Butt Joint

The technique applied here was also applied when using the BESWW sample (refer to Figure 2b.). The BESWW sample length was about 300 mm long with 10 mm gaps between channels. Compressive cyclic loading was applied to the sample at 322 Mpa (1.5 MN). When the pre-set alarm activated after 250,000 load cycles, the fatigue test was suspended immediately and the weld was thoroughly inspected by ultrasonic NDI and magnetic particle testing. The inspections identified a very fine crack on the weld surface at the time. This test demonstrated that the SMS sensor was sensitive enough to detect a very fine surface crack on a real weld surface.

4.9. Limitations of the Technique

It is already been identified the technique can only detect surface cracking. This can be a significant deficiency when cracking initiates beneath the surface. An additional limitation of the SMS sensor is that it can't accurately pinpoint the crack position. A few techniques to overcome this difficulty have been put forward by the sensor suppliers. One is to send coloured gas through the cracked channel so that if a leak occurs the location can be detected by sight. This technique will be studied separately.

4.10. Reduction in Vacuum Pressure

Another experiment was performed to determine the minimum vacuum pressure level that can be tolerated inside the channels. It would be of significant advantage to minimise the physical size of the vacuum source if the vacuum sensor system is used in a confined area. If a reduced vacuum level is required in the tubes, it follows that the size and energy of consumption of the pump can be reduced. To reduce the size of the pump however, the vacuum level needs to be drastically reduced. For example, if the vacuum level is reduced from 200 mBar to 10 mBar, one can replace the macro vacuum pump with a micro pump.

A micro pump is being developed by MPD using MEMS technology. In this case the controlling MEMS electronic circuitry can be minimised to match the vacuum pump size.

Next step in this program is to reduce the differential pressure monitor alarm level just above the noise level. The SIM alarm level has been reduced from 1.37 mbar to 0.5 mbar by reducing the pressure in steps of approximately 0.5 mbar. It was found that the alarm activation level can be safely reduced to 0.5 mbar, which is still much higher than signal noise generated by the surrounding environment. It is therefore implied that the alarm level threshold can be reduced to 0.5 mbar or below without signal noise affecting the output. For practical purposes, the noise level is under 0.15 mbar.

5. ADVANCED VACUUM-PRESSURE SENSOR UNDER DEVELOPMENT BY MPD

Miniturisation of the vacuum sensor would be advantageous particularly in locations where access to, and space around, a structural section is limited. For this reason, MPD is developing a minaturised vacuum sensor system . A micro pump will replace the vacuum source. The vacuum channels have been produced and fabricated using MEMS techniques, significantly reducing the width and the depth of channels to less than 100 μm . A simple IC circuit replaced the differential pressure monitor device with smart sensor with IC circuit. This part will be eventually coupled with the sensor. The basic concept of the minaturised sensor is shown in Figure 8.

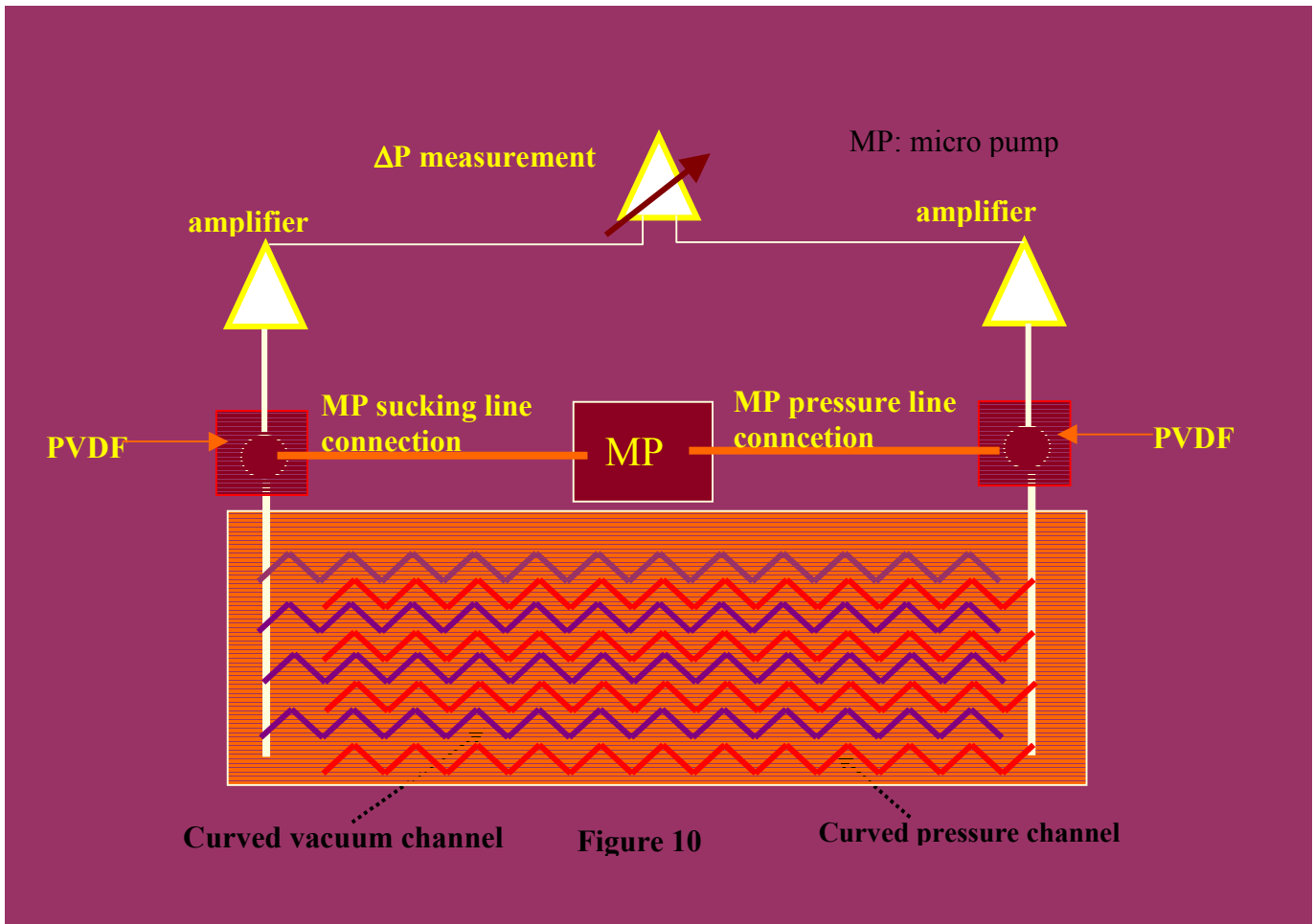


Figure 8.

6. CONCLUSIONS

- The vacuum sensor is sensitive to surface breaking defects and has been used to detect surface crack initiation and growth.
- The output data is only related to the change in pressure due to a volumetric change in the channel cavities, which is independent from factors such as variations in material, mechanical and electrical properties. For this reason, the sensor is free from all boundary conditions except the geometric effects.
- When a crack crosses a vacuum channel, one can measure the crack size and anticipate fracture type as well as fatigue life by studying the gradient between pressure variation and time,
- The SMS vacuum source can be replaced by a MEMS based micro pump if the dimensions of the vacuum channels can be reduced from 250 μm to less than 100 μm .

7. ACKNOWLEDGMENTS

These are given to a number of people who offered helpful advice and comments during the experiment, especially to Brian Dixon from MPD and Ken Davey from SMS company for the full financial and technical support.

8. REFERENCES

- [1]. Francesco Lanza di Scalea, Tobias P. Berndt, Robert E. Green, Jr. and B. Boro Djordjevic, *Advanced in Optical Methods for Non-Contact Non-destructive Evaluation*, American Institute of Physics Conference Proceedings, No 497, 1999, p149-55
- [2]. Alan A. Bakwer, Stephen C. Galea and Ian G. Powlesland, *A Smart Patch Approach for Bonded Composite Repair/Reinforcement of Primary Airframe Structures*. Proceedings of Second Joint NASA/FAA/DoD Conference on Aging Aircraft Williamsburg, Virginia, August 31-September 3, 1998, p328-338
- [3]. J.W. Dally and R.L. Sanford, *Strain-Gage Methods for Measuring the Opening-Mode Stress-Intensity Factor, K_I* , Experimental Mechanics, 1985, p381-388
- [4]. Prabhakar R. Marur, Hareesh V. Tippur, *A Strain Gage Method for Determination of Fracture Parameters in Bimaterial Systems*, Engineering Fracture Mechanics, Vol 64, 1999, p87-104
- [5]. Ken J. Davey, *Operating Instructions for the Davey System*; Amended 24-09-00, Structural Monitoring System Company, 1999.
- [6]. K.T.V. Grattan and B.T. Meggott, *Optical Fiber Sensor Technology*, Chapman & Hall, London, Glasgow, Weinheim. Newyork, Toyko, Melbourne, Madras, 1995
- [7]. W.W. Morey, G. Meltz, and W. H. Glenn, *Fiber Optic Bragg Grating Sensors*, SPIE, Vol 1169, Fiber Optic and Laser Sensors VII, 1989, p98-107
- [8]. Yun-Jiang rao, *In-Fibre Bragg Grating sensors (Review Article)*, Meas. Sci. Technology, Vol 8, 1997, p355-375
- [9]. C. Pardo De Vera and J.A. Gemes, *Embedded Self-Sensing Piezoelectric for Damage Detection*, *Journal of Intelligent Material Systems and Structures*, Vol 9 Nov, 1998, p876-882
- [10]. Fanping Sun and Craig A. Rogers, *Structural Frequency Response Function Acquisition vis Electric Impedance Measurement of Surface-Bonded Piezoelectric Sensor/Actuator*, American Institute of Aeronautics and Astronautics, 1995, p3450-3458.
- [11]. Chang-Qing Chen and Ya-Peng Shen, *Optical Control of Active Structures with Piezoelectric Modal Sensors and Actuators*, Smart Mater.Struc. Vol 6, 1997, p403-409
- [12]. S.S. Rao and M. Sunar, *Analysis of Distributed Thermopiezoelectric Sensors and Actuators in Advanced Intelligent Structures*, Vol 31 No 7, AIAA Journal, 1993, p1280-1286
- [13]. Erol Harvey, Phil T Rumsby, Malcolm C Gower, Jason L Remnant, *Microstructuring by Excimer Laser*, Vol 2639, SPIE, 1995, p266-277
- [14]. J Arnold, U Dashbach, W Ehrfeld, K Hesch and H Lowe. *Combination of Excimer Laser Micromachining and Replication Processes Suited for Large Scale Production*, Applied Surface Science, Vol 86, 1995, p251-258